

CLARIFICATION AS SUPERVISION: REINFORCEMENT LEARNING FOR VISION-LANGUAGE INTERFACES

005 **Anonymous authors**

006 Paper under double-blind review

ABSTRACT

011 Recent text-only models demonstrate remarkable reasoning capabilities.
 012 Extending these to visual domains requires vision-language models to trans-
 013 late images into text descriptions. However, current models, trained to
 014 produce captions for human readers, often omit the precise details that
 015 reasoning systems require. This creates an interface mismatch: reasoners
 016 often fail not due to reasoning limitations but because they lack access to
 017 critical visual information. We propose Adaptive-Clarification Reinforce-
 018 ment Learning (AC-RL), which teaches vision models what information
 019 reasoners need through interaction. Our key insight is that clarification re-
 020 quests during training reveal information gaps; by penalizing success that
 021 requires clarification, we create pressure for comprehensive initial captions
 022 that enable the reasoner to solve the problem in a single pass. AC-RL im-
 023 proves average accuracy by 4.4 points over pretrained baselines across seven
 024 visual reasoning benchmarks, and analysis shows it would cut clarification
 025 requests by up to 39% if those were allowed. By treating clarification as
 026 a form of implicit supervision, AC-RL demonstrates that vision-language
 027 interfaces can be effectively learned through interaction alone, without re-
 028 quiring explicit annotations.

1 INTRODUCTION

031 Recent advances in reinforcement learning have produced text-based reasoning models with
 032 remarkable **reasoning** capabilities (Guo et al., 2025a; Shao et al., 2024). While these rea-
 033 soning capabilities are impressive, extending them to visual domains requires careful con-
 034 sideration of how visual and linguistic information should interface.

035 Several recent works explore decoupled architectures for visual reasoning, where vision mod-
 036 ules translate images into text descriptions that are then processed by text-only reasoners
 037 (Chen et al., 2023; Zhou et al., 2024a; Gupta & Kembhavi, 2023). This modular paradigm
 038 **can offer practical advantages**: it enables reuse of existing text-only reasoning models with-
 039 out costly multimodal retraining, allows flexible composition of specialized components,
 040 and provides interpretable interfaces between perception and reasoning. **This decoupling**
 041 **is particularly relevant when powerful reasoners are available only through APIs that can-**
 042 **not be fine-tuned, or when reasoners are prohibitively expensive to fine-tune.** Furthermore,
 043 many domains have specialized vision-language models (e.g., for medical imaging (Li et al.,
 044 2023), web interfaces (Lee et al., 2023), or engineering diagrams (Doris et al., 2025)) but
 045 these models often lack the broader reasoning ability of text based models. This further
 046 motivates decoupling perception from reasoning, and learning the interface between them.
 047 Systems like COLA and ViCor demonstrate this approach, using LLMs as coordinators that
 048 operate on text descriptions of visual content (Chen et al., 2024). The common thread **in**
 049 **these approaches** is that visual information flows through a linguistic bottleneck, requiring
 050 careful design of what information to communicate (Singh et al., 2024; Guo et al., 2025c).

051 However, this decoupling creates a critical alignment challenge: vision-language tools must
 052 learn what visual information each specific reasoner requires for successful problem-solving.
 053 Vision-language models are typically trained on diverse multimodal datasets to produce
 descriptions sufficient for general visual understanding and question answering. Yet differ-

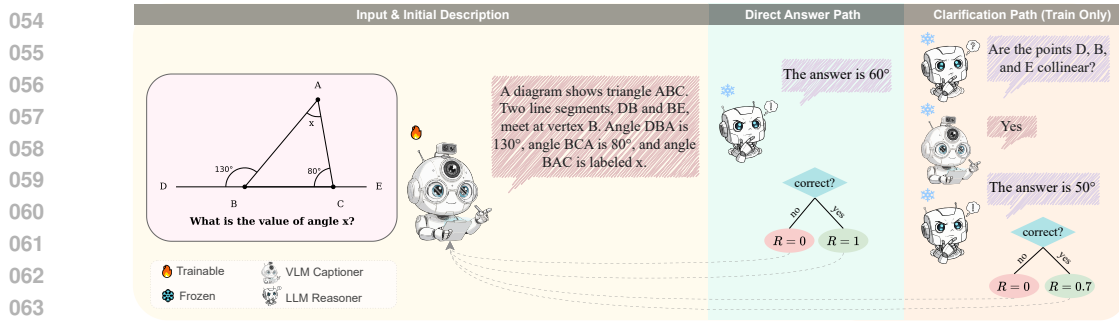


Figure 1: **Adaptive-Clarification Reinforcement Learning (AC-RL) training framework.** Given an image and a question, a trainable captioner (🔥) generates an initial description. During training, the frozen reasoner (❄️) evaluates whether this description contains sufficient detail to solve the problem. If yes (Direct Answer Path), it attempts to answer directly, receiving reward $R = 1$ for correct answers or $R = 0$ for incorrect ones. If the description lacks crucial information (Clarification Path), the reasoner requests specific details, which are provided by a frozen reference captioner (❄️). Correct answers after clarification receive partial reward $R = 0.7$, while incorrect answers receive $R = 0$. Gradients (dotted arrows) flow only through the initial caption generation, not through clarification responses. At inference, only the direct answer path is used: the model has learned to generate sufficiently detailed initial captions, eliminating the need for clarification.

ent reasoning models may have distinct information needs: one might excel with precise measurements, while another benefits from structural or topological descriptions. Traditional supervised approaches would require annotating “ideal captions” for each reasoner, an infeasible task given the diversity of visual reasoning problems and the implicit nature of reasoner preferences. Moreover, what constitutes an informative caption cannot be determined a priori; it emerges only through interaction with the reasoning model.

Reinforcement learning offers a natural framework for this interface learning problem, but applying it to vision-reasoner coordination is challenging. The primary difficulty lies in the sparsity of learning signals: when using binary task rewards, the vision model receives identical zero rewards whether its caption is completely inadequate or missing one crucial detail. Additionally, the large action space of language generation combined with sparse rewards leads to inefficient exploration, where most generated captions result in failure without providing informative gradients.

To overcome the limitations of this sparse reward signal, we introduce Adaptive-Clarification Reinforcement Learning (AC-RL), a framework that encourages vision–language models to produce captions aligned with the needs of a specific reasoner (Figure 1). The key idea is to make use of successful clarification during training: when the reasoner fails to solve a task directly but succeeds after a clarification exchange, this suggests that the initial caption contained partially useful information but was not complete. We assign partial credit to such clarification-based success but prefer solutions achieved on the first attempt, thereby creating optimization pressure for more informative initial captions. During training, clarification responses are generated by a frozen reference model, and gradients flow only through the initial caption. This ensures that the clarifier is not optimized and prevents the captioner from “hiding behind” a strong clarifier instead of learning to produce sufficiently informative initial captions. Over time, this leads the vision module to front-load relevant details into the initial caption, enabling single-pass inference without clarification at test time.

More specifically, AC-RL transforms sparse binary rewards into a tiered structure: full reward for direct success, partial reward (we used $\alpha = 0.7$) for success requiring clarification, and zero for failure. This densification serves dual purposes. First, it converts many zero-reward episodes into partially rewarded ones, providing a gradient signal when initial captions are nearly sufficient. Second, the penalty $(1 - \alpha)$ creates pressure to discover self-sufficient captioning strategies aligned with single-pass deployment. Through thousands of interactions, the vision model explores different description strategies, learning without ex-

108 plicit supervision what quantitative details, spatial relationships, or structural patterns this
 109 particular reasoner needs for solving a problem.

110 We evaluate AC-RL on visual reasoning benchmarks, chosen as a controlled testbed where
 111 clear ground truth enables clean measurement and strong text-only reasoners exist, isolating
 112 the vision-language interface as the primary bottleneck. Most of these benchmarks target
 113 different forms of mathematical reasoning (such as visual geometry, diagram interpretation,
 114 logic puzzles, or reasoning over plots and tables) yet some also extend beyond mathematics,
 115 including problems from chemistry, physics, and biology, e.g., MMMU (Yue et al., 2024).

116 The key contributions of our work are as follows:

- 118 • An exploration-based framework that enables vision-language models to discover
 119 through reinforcement learning what visual information a reasoner requires, adapting
 120 from human-caption pretraining without explicit supervision.
- 121 • A clarification-aware reward structure that uses interaction patterns as learning
 122 signals, allowing models to identify information gaps and iteratively improve their
 123 captioning strategies through trial and error.
- 124 • An empirical demonstration that our clarification-aware training scaffold effectively
 125 teaches captioners to anticipate reasoner needs, leading to improved accuracy on
 126 seven mathematical VQA benchmarks and a measurable reduction in clarification
 127 dependency at inference.

129 2 RELATED WORK

130 **131 Reinforcement learning for reasoning in language models.** Recent work shows RL
 132 can teach extended mathematical reasoning, with DeepSeek-R1 demonstrating learned poli-
 133 cies outperform prompt-based chain-of-thought (Guo et al., 2025a). Visual extensions em-
 134 ploy diverse strategies: training stability (Skywork-R1V2 (Wang et al., 2025b), Vision-R1
 135 (Huang et al., 2025)), replay mechanisms (VL-Rethinker (Wang et al., 2025a), OpenVL-
 136 Thinker (Deng et al., 2025)), and cross-modal formalization (R1-OneVision (Yang et al.,
 137 2025), Mulberry (Yao et al., 2024)). These methods focus on extending reasoning chains to
 138 handle visual inputs. We take an orthogonal approach by shaping the interface between per-
 139 ception and reasoning modules, using clarification-aware rewards to teach captioners what
 140 information reasoners need rather than how to reason about it.

141 **142 Decoupled perception–reasoning and interface design** Decoupling visual percep-
 143 tion from linguistic reasoning offers modularity and the ability to reuse strong text-only
 144 reasoners, but it raises an interface-alignment challenge: captions optimized for human
 145 readability may omit the quantitative and structural cues a reasoner needs (Zhou et al.,
 146 2024a; Guo et al., 2025c; Singh et al., 2024). Coordination frameworks use an LLM to route
 147 or aggregate information from one or more VLMs (e.g., COLA’s coordinator that queries
 148 complementary experts) (Chen et al., 2023), or to interleave “see-think-confirm” phases that
 149 explicitly ground and verify intermediate steps (VCTP) (Chen et al., 2024). Neuro-symbolic
 150 systems like VisProg sidestep monolithic pipelines by composing programs over off-the-shelf
 151 vision tools (Gupta & Kembhavi, 2023). Our approach adheres to the decoupled setup but
 152 replaces fixed protocols with an RL objective that learns, from interaction, which *caption*
 153 *features* best serve a specific reasoner.

154 **155 Learning alignment through interaction.** Several methods optimize captions specif-
 156 ically for reasoning rather than human readability. Most relevant to our work, RACRO
 157 directly uses binary task rewards to align a captioner to a reasoner (Gou et al., 2025),
 158 demonstrating that interface learning is possible through RL alone. However, RACRO re-
 159 lies solely on sparse binary rewards, which we show can be significantly improved through
 160 our clarification-aware tiered reward structure that densifies the learning signal. LAMOC
 161 and VLRM leverage language model feedback and VLM-as-reward-model, respectively (Du
 162 et al., 2023; Dzabraisev et al., 2024). OmniCaptioner generates long-context descriptions
 163 that improve LLM reasoning (Lu et al., 2025), while Critic-V employs a learned VLM critic

162 (Zhang et al., 2025). Beyond vision, multi-agent frameworks have shown that LLMs can
 163 coordinate through language-only protocols, and that adapting inputs to a solver’s biases
 164 can improve performance (Wu et al., 2024; Zhou et al., 2024b).

165

166

167 3 METHODOLOGY

168

169 3.1 THE VISION-REASONER INTERFACE PROBLEM

170

171 We consider a modular architecture where a trainable vision-language model, the captioner
 172 \mathcal{V}_θ , translates images into text descriptions that enable a frozen text-only model, the reasoner
 173 \mathcal{R} , to solve visual reasoning tasks. Given an image I and question Q , the system produces
 174 an answer A . The central challenge lies in learning what visual information the specific
 175 reasoner requires, without explicit supervision defining “ideal captions”.

176

177 We specifically target scenarios where the reasoner \mathcal{R} is frozen, reflecting deployment con-
 178 straints where the reasoning system cannot be modified (e.g., accessible only via an API).
 179 This makes the learning problem more challenging: the captioner must unilaterally adapt
 180 to a fixed target through interaction, with no co-adaptation to make the reasoner more
 181 accommodating.

182

183 Our approach leverages successful clarification as implicit supervision. When the reasoner
 184 fails to solve a task directly but succeeds after a clarification exchange, this suggests that
 185 the initial caption was partially informative: it must have provided enough context for
 186 the reasoner to identify what might be missing, formulate a meaningful follow-up question,
 187 and ultimately solve the problem. AC-RL captures this signal through a tiered reward
 188 structure: full reward for direct success, partial reward for success after clarification, and
 189 zero otherwise. Over time, the captioner learns to anticipate the kind of information that
 190 would otherwise be requested and to include it proactively in the initial description. This
 191 leads to progressively more informative captions and enables efficient single-pass inference
 192 without clarification at test time.

193

194

195 3.2 TRAINING AND INFERENCE PROTOCOLS

196

197 During training, we permit structured interaction between the captioner and reasoner. The
 198 captioner first generates an initial caption $c_0 \sim \pi_\theta(\cdot | I, Q)$ describing the visual content.
 199 The reasoner processes this caption and either produces an answer directly or requests
 200 clarification with a specific question q_1 . When clarification is requested, a *frozen reference*
 201 *model* π_{ref} provides the response $c_1 \sim \pi_{\text{ref}}(\cdot | I, Q, q_1)$. The reasoner then produces its final
 202 answer A using all available information.

203

204 Crucially, the clarification response comes from a frozen checkpoint that receives no gradients
 205 during training. This design ensures that the captioner cannot rely on improving clarification
 206 capabilities and must instead learn to front-load relevant information into the initial caption.
 207 Details of this protocol and the complete algorithm appear in Figure 1 and Appendix A.

208

209 At inference time, the system operates in a single pass: the captioner generates one descrip-
 210 tion $c_0 \sim \pi_\theta(\cdot | I, Q)$, and the reasoner must produce the answer based solely on this initial
 211 caption. This single-pass constraint is crucial for practical applications where multi-turn
 212 interaction would be computationally expensive or require architectural changes to existing
 213 tool-calling frameworks. By learning to front-load information during training, our approach
 214 produces captioners that work with standard single-pass inference. The reasoner processes
 215 the initial caption without needing to be modified to request clarifications.

216

217

218 3.3 CLARIFICATION-AWARE REWARD DESIGN

219

220

221 A key contribution of AC-RL is the tiered reward structure that densifies the learning signal.
 222 In standard reinforcement learning for visual question answering, episodes receive binary
 223 rewards based solely on answer correctness. This sparse signal provides limited feedback
 224 when the captioner produces nearly sufficient but incomplete descriptions.

216 Our reward function addresses this sparsity by distinguishing three outcomes:
 217

$$218 \quad R(\tau) = \begin{cases} 1 & \text{if correct answer without clarification} \\ 219 \quad \alpha & \text{if correct answer with clarification} \\ 220 \quad 0 & \text{if incorrect answer} \end{cases} \quad (1)$$

221 where $\alpha \in (0, 1)$ and τ denotes the complete episode trajectory. We set $\alpha = 0.7$.
 222

223 This structure serves dual purposes. First, it converts many zero-reward episodes into
 224 partially rewarded ones, providing gradient signal when the initial caption contains most but
 225 not all necessary information. This densification is particularly valuable early in training
 226 when captions frequently lack specific details. Second, the penalty $(1 - \alpha)$ for requiring
 227 clarification creates optimization pressure toward self-sufficient initial captions that align
 228 with single-pass deployment.

229 Clarification responses come from a frozen reference model rather than the training policy.
 230 This ensures gradients flow only through the initial caption, creating direct pressure to front-
 231 load information rather than rely on clarification quality. Problems beyond the reasoner’s
 232 capability contribute no gradient: when all caption variants for a problem receive zero
 233 reward, all advantages are zero and the problem is effectively ignored during optimization.

234 The clarification mechanism thus acts as a scaffold that provides intermediate credit assign-
 235 ment. Episodes where the reasoner would fail with the initial caption alone but succeeds
 236 after clarification receive partial reward, signaling that the caption was nearly adequate.
 237 This graded feedback enables more sample-efficient learning compared to binary rewards
 238 that treat all failures equivalently.

239 3.4 POLICY OPTIMIZATION

240 We optimize the captioner using a KL-regularized objective that balances task performance
 241 with proximity to the pretrained initialization:

$$243 \quad J(\theta) = \mathbb{E}_{(I, Q) \sim \mathcal{D}} [\mathbb{E}_{\tau \sim \pi_\theta}[R(\tau)]] - \beta \cdot D_{\text{KL}}(\pi_\theta \parallel \pi_{\text{ref}}) \quad (2)$$

244 where π_{ref} denotes a fixed reference policy for regularization.

245 We employ Beta-Normalization Policy Optimization (Xiao et al., 2025)¹, which is a variant
 246 of GRPO (Shao et al., 2024), an on-policy RL algorithm that optimize over groups of
 247 responses per prompt. Although rewards are assigned individually to each rollout A , the
 248 update is driven by relative performance across rollouts for the same task (I, Q) : only
 249 captions that perform strictly better than alternatives contribute a gradient. When all
 250 rollouts fail identically (including after clarification) no update is applied, preventing tasks
 251 unsolvable by the reasoner from penalizing otherwise potentially strong captions.

252 Importantly, gradients flow only through the initial caption generation c_0 . Neither the frozen
 253 reasoner \mathcal{R} nor the clarification model π_{ref} receive gradient updates, ensuring the captioner
 254 adapts unilaterally to the fixed reasoner’s preferences. We prove in Appendix B that our
 255 tiered reward preserves unbiasedness of the policy gradient estimator despite post-action
 256 stochasticity from the reasoner.

258 4 EXPERIMENTS

259 We evaluate whether Adaptive-Clarification Reinforcement Learning (AC-RL) successfully
 260 aligns vision-language models with the information needs of downstream reasoning systems.
 261 Our experimental design tests five key hypotheses: (1) AC-RL improves task performance
 262 compared to both pretrained models and standard reinforcement learning approaches (i.e.,
 263 learning with the tiered rewards and clarifications is beneficial), (2) the clarification-aware
 264 training scaffold contributes meaningfully to performance gains beyond standard RL, (3)
 265 the improvements stem from learning to front-load reasoner-relevant information into initial
 266 captions, (4) AC-RL is robust to the penalty α , and (5) generalizes to held-out reasoners.
 267

268 ¹BNPO fits a Beta distribution to the reward distribution within each prompt group, providing
 269 more stable advantage estimation for bounded rewards compared to standard normalization. Details
 are provided in Appendix A

270 **System Architecture.** We instantiate the trainable captioning policy with InternVL3-2B
 271 or Qwen2.5-VL-3B. Their modest size enables extensive RL experimentation and ablations,
 272 and when paired with a strong reasoner, they provide reliable baseline competence across
 273 the evaluated benchmarks. Their scale also makes GRPO optimization tractable without
 274 requiring extensive computational resources. The frozen reasoning system \mathcal{R} is DeepSeek-
 275 R1-Qwen-32B, a powerful text-only model trained for mathematical reasoning with par-
 276 ticularly strong instruction following capabilities. We also evaluate the vision models as
 277 standalone systems to quantify the benefits of architectural decoupling. We chose mathe-
 278 matical reasoning as our evaluation domain for two reasons: (1) clear ground truth enables
 279 clean measurement of interface improvements, and (2) strong text-only reasoners exist, iso-
 280 lating the vision-language interface as the bottleneck rather than reasoning capability.

281 **Training Configurations and Method Baselines** We compare four training config-
 282urations to isolate the effects of different design choices. The **Standalone VLM** baseline
 283 has the vision-language model answer questions directly without a separate reasoner. The
 284 **Pretrained + Reasoner** configuration pairs the pretrained VLM with the frozen reasoner
 285 without fine-tuning, measuring the immediate benefit of modular architectures. **Binary-**
 286 **Reward RL** fine-tunes the captioner with binary task success rewards, similarly to re-
 287 cent work, RACRO (Gou et al., 2025). Finally, **AC-RL** employs our tiered rewards and
 288 clarification-aware training scaffold. These baselines allow us to decompose gains from
 289 architectural decoupling, reinforcement learning, and our clarification-aware training scaffold.
 290 All RL methods are trained on ViRL-39K (Wang et al., 2025a), a visual instruction dataset
 291 focused on mathematical reasoning, with evaluation performed on held-out benchmarks.

292 **Training Protocol.** AC-RL training uses the clarification-aware scaffold detailed in Sec-
 293 tion 3. During training, the captioner generates $c_0 \sim \pi_\theta$, and if the reasoner requests clarifi-
 294 cation, a frozen reference policy provides the response. The tiered rewards ($R = 1$ for direct
 295 success, $R = 0.7$ with clarification, $R = 0$ for failure) create gradients only through the ini-
 296 tial caption. We optimize using BNPO with KL regularization. Notably, AC-RL maintains
 297 greater generation diversity than standard RL throughout training (Appendix D).

298 **Evaluation Protocol.** All models are evaluated using **single-pass evaluation**: the cap-
 299 tioner produces a description that the reasoner uses to generate a final answer, with no clar-
 300 ification permitted. This protocol ensures that performance gains reflect improved caption
 301 quality rather than multi-turn interaction benefits. For behavioral analyses in Section 4.3,
 302 we additionally conduct instrumented runs with **clarification-enabled evaluation** where
 303 clarification is allowed, to measure clarification patterns. We evaluate on seven benchmarks
 304 spanning diverse visual math reasoning challenges and compare against leading proprietary
 305 and open-weights models (details in Appendix C). We report exact-match accuracy using
 306 EvalScope (Team, 2024a) and VLMEvalKit (Duan et al., 2024).

309 4.1 OVERALL PERFORMANCE

310 Table 1 presents our results in the context of leading proprietary and open-weights models.
 311 We first note that small vision-language models achieve limited performance when solving
 312 problems directly: InternVL-2B and Qwen2.5-VL-3B reach only 32.4% and 34.6% average
 313 accuracy respectively as standalone systems. Simply pairing these models with a strong
 314 reasoner (Pretrained + Reasoner) improves performance to 39.3% and 39.0%, demon-
 315 strating the value of modular architectures. However, applying AC-RL yields the most gains.

316 With a Qwen2.5-VL-3B captioner, AC-RL improves the average accuracy from 39.0 to 43.4
 317 (+4.4 points), with substantial gains on robustness and vision-centric benchmarks like *Dyna-*
 318 *Math* (+10.6) and *Math Verse* (+5.2). The InternVL-2B captioner sees a similar +3.3 average
 319 point increase. These results, obtained under an identical single-pass protocol, demon-
 320 strate that AC-RL effectively aligns the captioning policy with the downstream reasoner’s needs.

321 While we observe minor regressions on WeMath (−0.7 to −1.5 points), this benchmark
 322 explicitly targets preexisting knowledge deficits rather than visual extraction. AC-RL’s op-
 323 timization pressure prioritizes precise visual details, yielding substantial gains on extraction-

324 heavy tasks like DynaMath and MathVerse. AC-RL excels at enabling reasoners to see more,
 325 but cannot address the reasoner’s internal knowledge gaps such as missing formulas, which
 326 limit WeMath performance.

328 Table 1: Main results on multi-modal reasoning benchmarks: MathVista (MVista), Math-
 329 Vision (MVision), MathVerse (MVerse), MMMU, WeMath (WeM), DynaMath (DynaM),
 330 and LogicVista (LVista). Our AC-RL method, evaluated in the final blocks for each model
 331 size, significantly enhances the performance of small vision models.

Model	MVista	MVision	MVerse	MMMU	WeM	DynaM	LVista	AVG
Proprietary Models								
GPT-4o-20241120	60.0	31.2	40.6	70.7	45.8	34.5	52.8	47.9
Gemini-2.0-Flash	70.4	43.6	47.7	72.6	47.4	42.1	52.3	53.7
Claude-3.7-Sonnet	66.8	41.9	46.7	75.0	49.3	39.7	58.2	53.9
o1	73.9	42.2	—	78.2	—	—	—	—
Gemini 2.5 Pro	80.9	69.1	76.9	74.7	78.0	56.3	73.8	72.8
Seed1.5-VL (Thinking)	79.5 [†]	68.7	—	77.9	77.5	—	—	75.9*
Open-Weights Models								
InternVL3-2B-MPO	57.0	21.7	25.3	48.6	22.4	14.6	36.9	32.4
InternVL3-8B-MPO	71.6	29.3	39.8	62.7	37.1	25.5	44.1	44.3
Ovis2-8B	71.8 [†]	25.9	42.3	59.0	—	—	39.4	47.7
InternVL3-14B-MPO	75.1	37.2	44.4	67.1	43.0	31.3	51.2	49.9
QVQ-72B-Preview	70.3	34.9	48.2	70.3	39.0	30.7	58.2	50.2
MMR1-Math-v0-7B	71.0 [†]	30.2	49.2	—	—	—	50.8	50.3
InternVL3-38B-MPO	75.1	34.2	48.2	70.1	48.6	35.3	58.4	52.8
VL-Rethinker-72B	80.3	43.9	—	68.8	—	—	—	—
InternVL3-78B-MPO	79.0	43.1	51.0	72.2	46.0	35.1	55.9	54.6
InternVL-2B								
Standalone VLM	57.0	21.9	25.3	48.6	22.4	14.6	36.9	32.4
Pretrained + Reasoner	61.0	34.7	28.9	57.4	32.8	12.0	48.3	39.3
AC-RL (ours)	65.3	36.7	36.8	58.4	32.1	20.0	49.0	42.6
	(+4.3)	(+2.0)	(+7.9)	(+1.0)	(-0.7)	(+8.0)	(+0.7)	(+3.3)
Qwen2.5-VL-3B								
Standalone VLM	64.5	21.9	28.8	50.1	24.2	13.4	39.6	34.6
Pretrained + Reasoner	59.7	32.8	29.2	55.2	34.7	14.2	47.2	39.0
AC-RL (ours)	63.8	36.8	34.4	57.7	33.2	24.8	53.0	43.4
	(+4.1)	(+4.0)	(+5.2)	(+2.5)	(-1.5)	(+10.6)	(+5.8)	(+4.4)

358 [†] Result on *testmini/minи* subset.

359 4.2 ABLATIONS

360 To better understand the source of these improvements, we analyze the incremental value
 361 of each component in our approach using the Qwen2.5-VL-3B model (Table 2). All config-
 362 urations are evaluated using direct inference (no clarification allowed).

363 4.2.1 DECOMPOSITION OF PERFORMANCE GAINS

364 Table 2: **Decomposition of performance gains on Qwen2.5-VL-3B** across multi-
 365 modal reasoning benchmarks: MathVista (MVista), MathVision (MVision), MathVerse
 366 (MVerse), MMMU, WeMath (WeM), DynaMath (DynaM), and LogicVista (LVista). All
 367 models are evaluated in a single-pass setting. The results show that AC-RL provides a
 368 significant performance boost beyond both architectural decoupling and Binary Rewards.

Training Method	MVista	MVision	MVerse	MMMU	WeM	DynaM	LVista	AVG
VLM-only (No Reasoner)	64.50	21.90	28.80	50.10	24.20	13.40	39.60	34.64
Decoupled (No RL)	59.69	32.80	29.18	55.22	34.71	14.17	47.20	39.00
Binary-Reward RL	62.60	34.30	31.09	55.44	33.45	17.56	47.42	40.27
AC-RL (Ours)	63.80	36.84	34.39	57.70	33.22	24.75	53.02	43.39

378 The results illustrate a clear progression. First, decoupling the captioner from the reasoner
 379 (Pretrained + Reasoner) yields substantial gains, particularly on structurally complex tasks
 380 like *MathVision* (21.9 → 32.8). Second, applying binary-reward RL provides further im-
 381 provements across most benchmarks. However, our clarification-aware AC-RL delivers the
 382 most substantial gains over Binary-Reward RL: *DynaMath* improves by +7.2 points (17.56
 383 → 24.75), *LogicVista* by +5.6 points, and *MathVerse* by +3.3 points.

384 The improvements on *DynaMath* are especially noteworthy. While Binary-Reward RL
 385 achieves modest gains over the pretrained baseline (+3.4 points), AC-RL delivers an ad-
 386 dditional +7.2 points, reaching 24.75% accuracy on the most challenging problem variants.
 387

388 4.2.2 SENSITIVITY TO CLARIFICATION PENALTY

389 The clarification penalty ($1 - \alpha$) controls the reward
 390 reduction for success requiring clarification. Table 3
 391 shows results across penalty values {0.1, 0.3, 0.5, 0.7}.
 392 Intermediate penalties (0.3, 0.5) consistently outper-
 393 form extremes, with near-identical *MathVision* per-
 394 formance (40.2 vs 40.1) demonstrating robustness.
 395 Penalties that are too weak (0.1) provide insuffi-
 396 cient optimization pressure, while too strong (0.7) ap-
 397 proaches binary rewards, losing partial credit benefits.
 398

399 4.2.3 GENERALIZATION ACROSS REASONERS

400 A natural question is whether learned
 401 strategies generalize or overfit to the train-
 402 ing reasoner. Table 4 compares caption-
 403 ers paired with DeepSeek-R1-0528-Qwen3-
 404 8B, differing in size and checkpoint from
 405 our training reasoner (DeepSeek-R1-Qwen-
 406 32B). With the training reasoner, AC-RL
 407 improves by +8.5 and +5.5 points on *Log-
 408 icVista* and *MathVision*. With the unseen reasoner, AC-RL achieves comparable gains
 409 (+8.7, +6.5), suggesting it learns generally useful captioning strategies rather than exploit-
 410 ing idiosyncrasies of the training reasoner.
 411

412 4.3 ANALYSIS OF INTERFACE BEHAVIOR

413 To understand the mechanism underlying AC-RL’s performance gains, we analyze how
 414 the training procedure modifies the captioner’s behavior. Our hypothesis is that the
 415 clarification-aware reward teaches the model to *front-load* reasoner-salient information into
 416 the initial caption, thereby reducing the need for clarification.
 417

418 We first measure the **clarification attempt rate** using clarification-enabled eval-
 419 uation (for measurement purposes only) and
 420 counting how frequently it requests clarifi-
 421 cation when processing captions from AC-
 422 RL-trained versus baseline models. Table 5
 423 shows that AC-RL dramatically reduces the
 424 frequency of clarification requests. On *MathVision*, the clarification rate drops from 40.69%
 425 (Binary-Reward RL baseline) to 28.95% (AC-RL). On *MathVerse*, the reduction is even
 426 more pronounced at 39%. This confirms that AC-RL-trained captioners learn to preemp-
 427 tively include information that would otherwise trigger follow-up questions.
 428

429 Building on this evidence, we compute the **clarification gap**: the difference in accuracy
 430 between clarification-enabled evaluation and single-pass evaluation. A smaller gap indi-
 431 cates that the initial caption is more informationally self-sufficient. Table 6 presents these
 432 results. For the baseline model, allowing clarification provides substantial accuracy gains:

Table 3: Sensitivity to the clarifica-
 tion penalty ($1 - \alpha$).

Penalty	LVista	MVision
0.1	53.2	35.8
0.3	55.7	40.2
0.5	52.4	40.1
0.7	50.1	35.5

Table 4: Cross-reasoner generalization.

Captioner	Reasoner	LVista	MVision
Pretrained	Train (32B)	47.2	34.7
AC-RL	Train (32B)	55.7	40.2
Pretrained	Unseen (8B)	44.3	30.0
AC-RL	Unseen (8B)	53.0	36.5

Table 5: Clarification attempt rate (%).

	MathVision	MathVerse
Binary Reward	40.7	49.6
AC-RL	29.0	30.3
Reduction	29%	39%

+2.89 points on MathVision and +4.06 points on MathVerse. In contrast, the AC-RL model shows minimal benefit from clarification and even a negative gap on MathVerse (-2.54), suggesting that its initial captions are so well-aligned that additional clarification can sometimes introduce noise. The relative improvement metric (fraction of previously incorrect answers that become correct with clarification) further confirms this pattern: AC-RL achieves 1.5% relative improvement on MathVision versus 4.4% for the baseline.

Table 6: Performance gap between clarification-enabled and single-pass evaluation. “Rel” denotes the fraction of previously incorrect answers that become correct when clarification is allowed. Smaller gaps indicate greater self-sufficiency of initial captions.

Dataset	Model	Clarification-Enabled	Single-Pass	Gap (Abs / Rel)
MathVision	AC-RL	37.66%	36.71%	+0.95 / 0.015
	Binary-Reward	37.20%	34.31%	+2.89 / 0.044
MathVerse_MINI	AC-RL	34.26%	36.80%	-2.54 / -0.040
	Binary-Reward	35.15%	31.09%	+4.06 / 0.059

Finally, to assess whether clarification requests are genuinely necessary, we measure accuracy under **denied clarification**: we identify instances where the model requested clarification during clarification-enabled evaluation, then examine the single-pass accuracy on this same subset (equivalent to denying the clarification request). The drop $\Delta_{\text{deny}} = \text{Acc}_{\text{clarification-enabled}} - \text{Acc}_{\text{denied}}$ quantifies how much the model relies on clarification when it requests it. Table 7 shows that while AC-RL reduces overall clarification frequency, its remaining requests are more selective. The AC-RL model exhibits a larger performance drop when clarification is denied ($\Delta_{\text{deny}} = 14.21$ on MathVision versus 11.43 for the baseline), despite making fewer requests overall (880 versus 1,237). This suggests that AC-RL learns to distinguish between recoverable and irrecoverable information gaps: it produces self-sufficient captions when possible, but when it does request clarification, these requests target instances where critical visual details cannot be inferred from context alone.

Table 7: Accuracy impact of denying clarification on instances where it was requested. Acc_{deny} is computed on the subset of problems where the reasoner requested clarification during clarification-enabled evaluation; for these specific problems, we measure accuracy using only the initial caption (i.e., denying the clarification request).

Dataset	Model	# Requests	Acc _{single-pass}	Acc _{deny} / Δ_{deny}
MathVision	AC-RL	880	36.71%	22.50% / 14.21
	Binary-Reward	1237	34.31%	22.88% / 11.43
MathVerse_MINI	AC-RL	276	36.80%	33.33% / 3.47
	Binary-Reward	496	31.09%	28.43% / 2.66

4.4 SUBJECT-LEVEL PERFORMANCE ANALYSIS

To better understand the nature of these improvements, we conduct a fine-grained analysis of performance across different mathematical subjects and difficulty levels. This reveals whether the model is generically improving or learning to prioritize specific types of information relevant to the reasoner. We decompose the MathVision and DynaMath benchmarks by subject area and compute per-subject accuracy for both the AC-RL model and the pretrained baseline (Qwen2.5-VL-3B + Reasoner configuration). Additionally, we analyze DynaMath average performance stratified by education level (elementary, high school, undergraduate) to assess whether AC-RL’s benefits vary with problem complexity.

Figure 2 visualizes the per-subject performance comparison. The analysis reveals that AC-RL’s gains are concentrated in subjects that depend heavily on precise quantitative and structural information. On MathVision, we observe the largest improvements in metric geometry for angles (+10.4 points), transformation geometry (+8.3 points), and algebra (+7.5 points). DynaMath shows even more pronounced gains in solid geometry (+18.7 points), algebra (+15.1 points), and puzzle tests (+13.5 points). These subjects arguably

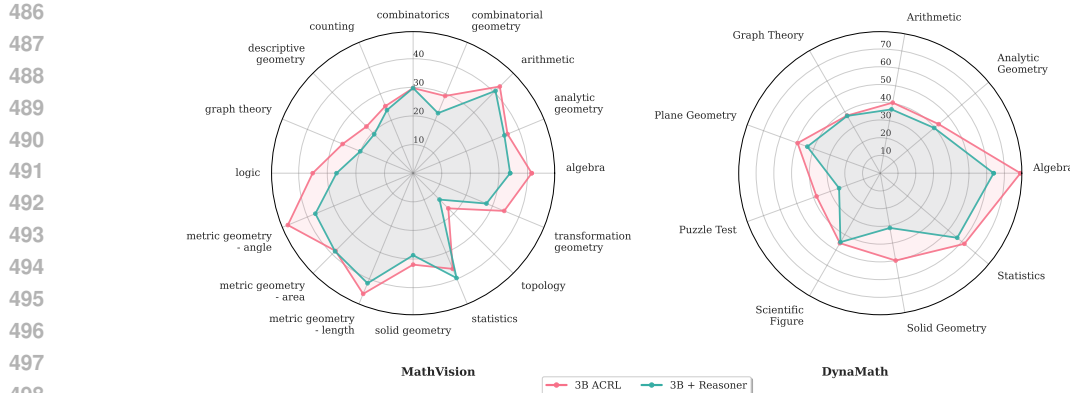


Figure 2: Subject-level performance comparing AC-RL to the pretrained baseline using Qwen2.5-VL-3B + Reasoner. Left: MathVision subjects. Right: DynaMath categories. AC-RL shows targeted improvements in quantitatively-intensive.

require extracting specific numerical values, spatial relationships, or structural patterns from images. In contrast, performance differences are minimal in subjects that rely more on general visual understanding or pattern recognition.

Figure 3 shows that AC-RL maintains consistent improvements across all difficulty levels on DynaMath. The absolute gains remain relatively stable at 6.5, 6.3, and 4.3 points for elementary, high school, and undergraduate levels, respectively. While both models show expected degradation as problem complexity increases, AC-RL preserves its advantage by learning to extract critical visual details needed at each level. The smaller gain at the undergraduate level may reflect inherent limits in what visual information alone can contribute to abstract problems.

This non-uniform improvement pattern indicates that AC-RL learns to extract and prioritize the specific types of information most valuable to the downstream reasoner. The selective nature of these improvements suggests that the clarification-aware training identifies and addresses systematic information gaps in the original captioning policy, with the model discovering domain-specific extraction strategies through interaction rather than explicit supervision.

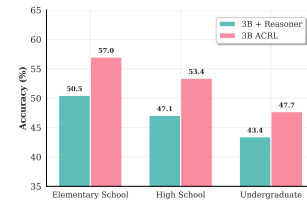


Figure 3: DynaMath average accuracy across education levels. AC-RL consistently outperforms the baseline regardless of problem difficulty.

5 CONCLUSION

We presented Adaptive-Clarification Reinforcement Learning (AC-RL), a framework that learns vision-reasoner interfaces through interaction rather than supervision. By using clarification requests as implicit feedback and tiered rewards, AC-RL enables captioners to discover what information their paired reasoner requires without explicit annotation. Our experiments demonstrate consistent improvements across seven mathematical reasoning benchmarks, with particularly strong gains on quantitatively-intensive domains.

The success of AC-RL suggests that interface alignment between AI modules can be learned through reinforcement learning without requiring explicit caption annotations. We demonstrated this on mathematical reasoning as a controlled testbed where clear ground truth enables clean measurement. The core mechanism of penalizing clarification-dependent success to encourage information front-loading could naturally extend to other settings where specialized VLMs interface with frozen reasoners, such as medical imaging (Li et al., 2023) or engineering diagrams (Doris et al., 2025); we leave empirical validation of such extensions for future work. Other promising directions include bidirectional adaptation where both modules co-evolve, using clarification content (not just occurrence) as richer supervision, and multi-turn clarification with decaying rewards for iterative refinement.

540 REFERENCES
541

542 Josh Achiam, Steven Adler, Sandhini Agarwal, Lama Ahmad, Ilge Akkaya, Florencia Leoni
543 Aleman, Diogo Almeida, Janko Altenschmidt, Sam Altman, Shyamal Anadkat, et al.
544 Gpt-4 technical report. *arXiv preprint arXiv:2303.08774*, 2023.

545 Shuai Bai, Keqin Chen, Xuejing Liu, Jialin Wang, Wenbin Ge, Sibo Song, Kai Dang, Peng
546 Wang, Shijie Wang, Jun Tang, Humen Zhong, Yuanzhi Zhu, Mingkun Yang, Zhaohai Li,
547 Jianqiang Wan, Pengfei Wang, Wei Ding, Zheren Fu, Yiheng Xu, Jiabo Ye, Xi Zhang,
548 Tianbao Xie, Zesen Cheng, Hang Zhang, Zhibo Yang, Haiyang Xu, and Junyang Lin.
549 Qwen2.5-vl technical report, 2025. URL <https://arxiv.org/abs/2502.13923>.

550 Liangyu Chen, Bo Li, Sheng Shen, Jingkang Yang, Chunyuan Li, Kurt Keutzer, Trevor
551 Darrell, and Ziwei Liu. Large language models are visual reasoning coordinators. In
552 *Thirty-seventh Conference on Neural Information Processing Systems*, 2023. URL <https://openreview.net/forum?id=1q0feiJ2i4>.

553 Zhenfang Chen, Qinhong Zhou, Yikang Shen, Yining Hong, Zhiqing Sun, Dan Gutfreund,
554 and Chuang Gan. Visual chain-of-thought prompting for knowledge-based visual rea-
555 soning. *Proceedings of the AAAI Conference on Artificial Intelligence*, 38(2):1254–1262,
556 Mar. 2024. doi: 10.1609/aaai.v38i2.27888. URL <https://ojs.aaai.org/index.php/AAAI/article/view/27888>.

557 Gheorghe Comanici, Eric Bieber, Mike Schaeckermann, Ice Pasupat, Noveen Sachdeva, In-
558 derjit Dhillon, Marcel Blstein, Ori Ram, Dan Zhang, Evan Rosen, et al. Gemini 2.5:
559 Pushing the frontier with advanced reasoning, multimodality, long context, and next gen-
560 eration agentic capabilities. *arXiv preprint arXiv:2507.06261*, 2025.

561 Yihe Deng, Hritik Bansal, Fan Yin, Nanyun Peng, Wei Wang, and Kai-Wei Chang. Open-
562 vltthinker: Complex vision-language reasoning via iterative sft-rl cycles, 2025. URL
563 <https://arxiv.org/abs/2503.17352>.

564 Anna C Doris, Md Ferdous Alam, Amin Heyrani Nobari, and Faez Ahmed. Cad-coder:
565 An open-source vision-language model for computer-aided design code generation. In
566 *International Design Engineering Technical Conferences and Computers and Infor-
567 mation in Engineering Conference*, volume 89220, pp. V03AT03A031. American Society of
568 Mechanical Engineers, 2025.

569 Yifan Du, Junyi Li, Tianyi Tang, Wayne Xin Zhao, and Ji-Rong Wen. Zero-shot visual
570 question answering with language model feedback. *arXiv preprint arXiv:2305.17006*,
571 2023.

572 Haodong Duan, Junming Yang, Yuxuan Qiao, Xinyu Fang, Lin Chen, Yuan Liu, Xiaoyi
573 Dong, Yuhang Zang, Pan Zhang, Jiaqi Wang, et al. Vlmevalkit: An open-source toolkit
574 for evaluating large multi-modality models. In *Proceedings of the 32nd ACM International
575 Conference on Multimedia*, pp. 11198–11201, 2024.

576 Maksim Dzabraev, Alexander Kunitsyn, and Andrei Ivaniuta. Vlrm: Vision-language mod-
577 els act as reward models for image captioning. *arXiv preprint arXiv:2404.01911*, 2024.

578 Yunhao Gou, Kai Chen, Zhili Liu, Lanqing Hong, Xin Jin, Zhenguo Li, James T. Kwok, and
579 Yu Zhang. Perceptual decoupling for scalable multi-modal reasoning via reward-optimized
580 captioning, 2025. URL <https://arxiv.org/abs/2506.04559>.

581 Daya Guo, Dejian Yang, Haowei Zhang, Junxiao Song, Peiyi Wang, Qihao Zhu, Runxin
582 Xu, Ruoyu Zhang, Shirong Ma, Xiao Bi, et al. Deepseek-r1 incentivizes reasoning in llms
583 through reinforcement learning. *Nature*, 645(8081):633–638, 2025a.

584 Dong Guo, Faming Wu, Feida Zhu, Fuxing Leng, Guang Shi, Haobin Chen, Haoqi Fan, Jian
585 Wang, Jianyu Jiang, Jiawei Wang, Jingji Chen, Jingjia Huang, Kang Lei, Liping Yuan,
586 Lishu Luo, Pengfei Liu, Qinghao Ye, Rui Qian, Shen Yan, Shixiong Zhao, Shuai Peng,
587 Shuangye Li, Sihang Yuan, Sijin Wu, Tianheng Cheng, Weiwei Liu, Wenqian Wang,
588 Xianhan Zeng, Xiao Liu, Xiaobo Qin, Xiaohan Ding, Xiaojun Xiao, Xiaoying Zhang,
589

594 Xuanwei Zhang, Xuehan Xiong, Yanghua Peng, Yangrui Chen, Yanwei Li, Yanxu Hu,
 595 Yi Lin, Yiyuan Hu, Yiyuan Zhang, Youbin Wu, Yu Li, Yudong Liu, Yue Ling, Yujia
 596 Qin, Zanbo Wang, Zhiwu He, Aoxue Zhang, Bairen Yi, Bencheng Liao, Can Huang, Can
 597 Zhang, Chaorui Deng, Chaoyi Deng, Cheng Lin, Cheng Yuan, Chenggang Li, Chenhui
 598 Gou, Chenwei Lou, Chengzhi Wei, Chundian Liu, Chunyuan Li, Deyao Zhu, Donghong
 599 Zhong, Feng Li, Feng Zhang, Gang Wu, Guodong Li, Guohong Xiao, Haibin Lin, Haihua
 600 Yang, Haoming Wang, Heng Ji, Hongxiang Hao, Hui Shen, Huixia Li, Jiahao Li, Jialong
 601 Wu, Jianhua Zhu, Jianpeng Jiao, Jiashi Feng, Jiaze Chen, Jianhui Duan, Jihao Liu,
 602 Jin Zeng, Jingqun Tang, Jingyu Sun, Joya Chen, Jun Long, Junda Feng, Junfeng Zhan,
 603 Junjie Fang, Junting Lu, Kai Hua, Kai Liu, Kai Shen, Kaiyuan Zhang, Ke Shen, Ke Wang,
 604 Keyu Pan, Kun Zhang, Kunchang Li, Lanxin Li, Lei Li, Lei Shi, Li Han, Liang Xiang,
 605 Liangqiang Chen, Lin Chen, Lin Li, Lin Yan, Liying Chi, Longxiang Liu, Mengfei Du,
 606 Mingxuan Wang, Ningxin Pan, Peibin Chen, Pengfei Chen, Pengfei Wu, Qingqing Yuan,
 607 Qingyao Shuai, Qiuyan Tao, Renjie Zheng, Renrui Zhang, Ru Zhang, Rui Wang, Rui
 608 Yang, Rui Zhao, Shaoqiang Xu, Shihao Liang, Shipeng Yan, Shu Zhong, Shuaishuai
 609 Cao, Shuangzhi Wu, Shufan Liu, Shuhan Chang, Songhua Cai, Tenglong Ao, Tianhao
 610 Yang, Tingting Zhang, Wanjun Zhong, Wei Jia, Wei Weng, Weihao Yu, Wenhao Huang,
 611 Wenjia Zhu, Wenli Yang, Wenzhi Wang, Xiang Long, XiangRui Yin, Xiao Li, Xiaolei Zhu,
 612 Xiaoying Jia, Xijin Zhang, Xin Liu, Xinchen Zhang, Xinyu Yang, Xiongcai Luo, Xiuli
 613 Chen, Xuantong Zhong, Xuefeng Xiao, Xujing Li, Yan Wu, Yawei Wen, Yifan Du, Yihao
 614 Zhang, Yining Ye, Yonghui Wu, Yu Liu, Yu Yue, Yufeng Zhou, Yufeng Yuan, Yuhang
 615 Xu, Yuhong Yang, Yun Zhang, Yunhao Fang, Yuntao Li, Yurui Ren, Yuwen Xiong, Zehua
 616 Hong, Zehua Wang, Zewei Sun, Zeyu Wang, Zhao Cai, Zhaoyue Zha, Zhecheng An,
 617 Zhehui Zhao, Zhengzhuo Xu, Zhipeng Chen, Zhiyong Wu, Zhuofan Zheng, Zihao Wang,
 618 Zilong Huang, Ziyu Zhu, and Zuquan Song. Seed1.5-vl technical report, 2025b. URL
 619 <https://arxiv.org/abs/2505.07062>.
 620 Zixian Guo, Ming Liu, Qilong Wang, Zhilong Ji, Jinfeng Bai, Lei Zhang, and Wangmeng
 621 Zuo. Integrating visual interpretation and linguistic reasoning for math problem solving,
 622 2025c. URL <https://arxiv.org/abs/2505.17609>.
 623 Tanmay Gupta and Aniruddha Kembhavi. Visual programming: Compositional visual
 624 reasoning without training. In *Proceedings of the IEEE/CVF conference on computer*
 625 *vision and pattern recognition*, pp. 14953–14962, 2023.
 626 Edward J Hu, Phillip Wallis, Zeyuan Allen-Zhu, Yuanzhi Li, Shean Wang, Lu Wang, Weizhu
 627 Chen, et al. Lora: Low-rank adaptation of large language models. In *International*
 628 *Conference on Learning Representations*.
 629 Wenxuan Huang, Bohan Jia, Zijie Zhai, Shaosheng Cao, Zheyu Ye, Fei Zhao, Zhe Xu, Yao
 630 Hu, and Shaohui Lin. Vision-r1: Incentivizing reasoning capability in multimodal large
 631 language models. *arXiv preprint arXiv:2503.06749*, 2025.
 632 Aaron Jaech, Adam Kalai, Adam Lerer, Adam Richardson, Ahmed El-Kishky, Aiden Low,
 633 Alec Helyar, Aleksander Madry, Alex Beutel, Alex Carney, et al. Openai o1 system card.
 634 *arXiv preprint arXiv:2412.16720*, 2024.
 635 Kenton Lee, Mandar Joshi, Iulia Raluca Turc, Hexiang Hu, Fangyu Liu, Julian Martin
 636 Eisenschlos, Urvashi Khandelwal, Peter Shaw, Ming-Wei Chang, and Kristina Toutanova.
 637 Pix2struct: Screenshot parsing as pretraining for visual language understanding. In *In-*
 638 *ternational Conference on Machine Learning*, pp. 18893–18912. PMLR, 2023.
 639 Chunyuan Li, Cliff Wong, Sheng Zhang, Naoto Usuyama, Haotian Liu, Jianwei Yang, Tris-
 640 tan Naumann, Hoifung Poon, and Jianfeng Gao. Llava-med: Training a large language-
 641 and-vision assistant for biomedicine in one day. *Advances in Neural Information Process-
 642 ing Systems*, 36:28541–28564, 2023.
 643 Pan Lu, Hritik Bansal, Tony Xia, Jiacheng Liu, Chunyuan Li, Hannaneh Hajishirzi, Hao
 644 Cheng, Kai-Wei Chang, Michel Galley, and Jianfeng Gao. Mathvista: Evaluating math-
 645 ematical reasoning of foundation models in visual contexts. In *International Conference*
 646 *on Learning Representations (ICLR)*, 2024a.

648 Shiyin Lu, Yang Li, Qing-Guo Chen, Zhao Xu, Weihua Luo, Kaifu Zhang, and Han-
 649 Jia Ye. Ovis: Structural embedding alignment for multimodal large language model.
 650 *arXiv:2405.20797*, 2024b.

651 Yiting Lu, Jiakang Yuan, Zhen Li, Shitian Zhao, Qi Qin, Xinyue Li, Le Zhuo, Licheng
 652 Wen, Dongyang Liu, Yuewen Cao, Xiangchao Yan, Xin Li, Tianshuo Peng, Shufei Zhang,
 653 Botian Shi, Tao Chen, Zhibo Chen, Lei Bai, Peng Gao, and Bo Zhang. Omnicaptioner:
 654 One captioner to rule them all, 2025. URL <https://arxiv.org/abs/2504.07089>.

655 Runqi Qiao, Qiuna Tan, Guanting Dong, Minhui Wu, Chong Sun, Xiaoshuai Song, Zhuoma
 656 GongQue, Shanglin Lei, Zhe Wei, Miaoqian Zhang, et al. We-math: Does your
 657 large multimodal model achieve human-like mathematical reasoning? *arXiv preprint*
 658 *arXiv:2407.01284*, 2024.

659 Zhihong Shao, Peiyi Wang, Qihao Zhu, Runxin Xu, Junxiao Song, Xiao Bi, Haowei Zhang,
 660 Mingchuan Zhang, YK Li, Yang Wu, et al. Deepseekmath: Pushing the limits of mathe-
 661 matical reasoning in open language models. *arXiv preprint arXiv:2402.03300*, 2024.

662 Jiaxi Li, Hao Zhang, Zhiqiang Hu, Boqiang Zhang, Hang Zhang, Yuming Jiang, Xin Li, Deli Zhao,
 663 Fan Wang, Yu Rong, Aixin Sun, Shijian Lu, Sicong Leng, Jing Wang. Mmr1: Advancing
 664 the frontiers of multimodal reasoning. <https://github.com/LengSicong/MMR1>, 2025.

665 Ayush Singh, Mansi Gupta, Shivank Garg, Abhinav Kumar, and Vansh Agrawal. Beyond
 666 captioning: Task-specific prompting for improved vlm performance in mathematical rea-
 667 soning, 2024. URL <https://arxiv.org/abs/2410.05928>.

668 Gemini Team, Rohan Anil, Sébastien Borgeaud, Jean-Baptiste Alayrac, Jiahui Yu, Radu
 669 Soricut, Johan Schalkwyk, Andrew M Dai, Anja Hauth, Katie Millican, et al. Gemini: a
 670 family of highly capable multimodal models. *arXiv preprint arXiv:2312.11805*, 2023.

671 ModelScope Team. EvalScope: Evaluation framework for large models, 2024a. URL <https://github.com/modelscope/evalscope>.

672 Qwen Team. Qvq: To see the world with wisdom, December 2024b. URL <https://qwenlm.github.io/blog/qvq-72b-preview/>.

673 Leandro von Werra, Younes Belkada, Lewis Tunstall, Edward Beeching, Tristan Thrush,
 674 Nathan Lambert, Shengyi Huang, Kashif Rasul, and Quentin Gallouédec. Trl: Trans-
 675 former reinforcement learning. <https://github.com/huggingface/trl>, 2020.

676 Haozhe Wang, Chao Qu, Zuming Huang, Wei Chu, Fangzhen Lin, and Wenhui Chen. Vi-
 677 rethinker: Incentivizing self-reflection of vision-language models with reinforcement learn-
 678 ing. *arXiv preprint arXiv:2504.08837*, 2025a.

679 Ke Wang, Junting Pan, Weikang Shi, Zimu Lu, Houxing Ren, Aojun Zhou, Mingjie
 680 Zhan, and Hongsheng Li. Measuring multimodal mathematical reasoning with math-
 681 vision dataset. In *The Thirty-eight Conference on Neural Information Processing Sys-
 682 tems Datasets and Benchmarks Track*, 2024. URL <https://openreview.net/forum?id=QWTCCxMpPA>.

683 Peiyu Wang, Yichen Wei, Yi Peng, Xiaokun Wang, Weijie Qiu, Wei Shen, Tianyidan Xie,
 684 Jiangbo Pei, Jianhao Zhang, Yunzhuo Hao, et al. Skywork r1v2: Multimodal hybrid
 685 reinforcement learning for reasoning. *arXiv preprint arXiv:2504.16656*, 2025b.

686 Qingyun Wu, Gagan Bansal, Jieyu Zhang, Yiran Wu, Beibin Li, Erkang Zhu, Li Jiang,
 687 Xiaoyun Zhang, Shaokun Zhang, Jiale Liu, Ahmed Hassan Awadallah, Ryen W White,
 688 Doug Burger, and Chi Wang. Autogen: Enabling next-gen LLM applications via multi-
 689 agent conversations. In *First Conference on Language Modeling*, 2024. URL <https://openreview.net/forum?id=BAakY1hNKS>.

690 Changyi Xiao, Mengdi Zhang, and Yixin Cao. Bnpo: Beta normalization policy optimiza-
 691 tion, 2025. URL <https://arxiv.org/abs/2506.02864>.

702 Yijia Xiao, Edward Sun, Tianyu Liu, and Wei Wang. Logicvista: Multimodal llm logical
 703 reasoning benchmark in visual contexts. *arXiv preprint arXiv:2407.04973*, 2024.

704

705 Yi Yang, Xiaoxuan He, Hongkun Pan, Xiyan Jiang, Yan Deng, Xingtao Yang, Haoyu Lu,
 706 Dacheng Yin, Fengyun Rao, Minfeng Zhu, et al. R1-onevision: Advancing generalized mul-
 707 timodal reasoning through cross-modal formalization. *arXiv preprint arXiv:2503.10615*,
 708 2025.

709 Huanjin Yao, Jiaxing Huang, Wenhao Wu, Jingyi Zhang, Yibo Wang, Shunyu Liu, Yingjie
 710 Wang, Yuxin Song, Haocheng Feng, Li Shen, and Dacheng Tao. Mulberry: Empowering
 711 mllm with o1-like reasoning and reflection via collective monte carlo tree search. *CoRR*,
 712 abs/2412.18319, 2024. URL <https://doi.org/10.48550/arXiv.2412.18319>.

713

714 Xiang Yue, Yuansheng Ni, Kai Zhang, Tianyu Zheng, Ruqi Liu, Ge Zhang, Samuel Stevens,
 715 Dongfu Jiang, Weiming Ren, Yuxuan Sun, Cong Wei, Botao Yu, Ruibin Yuan, Renliang
 716 Sun, Ming Yin, Boyuan Zheng, Zhenzhu Yang, Yibo Liu, Wenhao Huang, Huan Sun,
 717 Yu Su, and Wenhui Chen. Mmmu: A massive multi-discipline multimodal understanding
 718 and reasoning benchmark for expert agi. In *Proceedings of CVPR*, 2024.

719

720 Di Zhang, Jingdi Lei, Junxian Li, Xunzhi Wang, Yujie Liu, Zonglin Yang, Jiatong Li, Weida
 721 Wang, Suorong Yang, Jianbo Wu, et al. Critic-v: Vlm critics help catch vlm errors in
 722 multimodal reasoning. In *Proceedings of the Computer Vision and Pattern Recognition
 Conference*, pp. 9050–9061, 2025.

723

724 Renrui Zhang, Dongzhi Jiang, Yichi Zhang, Haokun Lin, Ziyu Guo, Pengshuo Qiu, Aojun
 725 Zhou, Pan Lu, Kai-Wei Chang, Yu Qiao, et al. Mathverse: Does your multi-modal llm
 726 truly see the diagrams in visual math problems? In *European Conference on Computer
 Vision*, pp. 169–186. Springer, 2024.

727

728 Kaiwen Zhou, Kwonjoon Lee, Teruhisa Misu, and Xin Wang. ViCor: Bridging visual un-
 729 derstanding and commonsense reasoning with large language models. In Lun-Wei Ku,
 730 Andre Martins, and Vivek Srikumar (eds.), *Findings of the Association for Com-
 731 putational Linguistics: ACL 2024*, pp. 10783–10795, Bangkok, Thailand, August 2024a. As-
 732 sociation for Computational Linguistics. doi: 10.18653/v1/2024.findings-acl.640. URL
<https://aclanthology.org/2024.findings-acl.640/>.

733

734 Yue Zhou, Yada Zhu, Diego Antognini, Yoon Kim, and Yang Zhang. Paraphrase and solve:
 735 Exploring and exploiting the impact of surface form on mathematical reasoning in large
 736 language models. In Kevin Duh, Helena Gomez, and Steven Bethard (eds.), *Proceedings
 737 of the 2024 Conference of the North American Chapter of the Association for Com-
 738 putational Linguistics: Human Language Technologies (Volume 1: Long Papers)*, pp.
 739 2793–2804, Mexico City, Mexico, June 2024b. Association for Computational Linguistics.
 740 doi: 10.18653/v1/2024.naacl-long.153. URL [https://aclanthology.org/2024.
 naacl-long.153/](https://aclanthology.org/2024.

 naacl-long.153/).

741

742 Jinguo Zhu, Weiyun Wang, Zhe Chen, Zhaoyang Liu, Shenglong Ye, Lixin Gu, Hao Tian,
 743 Yuchen Duan, Weijie Su, Jie Shao, et al. Internvl3: Exploring advanced training and
 744 test-time recipes for open-source multimodal models. *arXiv preprint arXiv:2504.10479*,
 745 2025.

746

747 Chengke Zou, Xingang Guo, Rui Yang, Junyu Zhang, Bin Hu, and Huan Zhang. Dynamath:
 748 A dynamic visual benchmark for evaluating mathematical reasoning robustness of vision
 749 language models. In *The Thirteenth International Conference on Learning Representa-
 750 tions*, 2025. URL <https://openreview.net/forum?id=VOAMTA8jKu>.

751

752

753

754

755

756 A AC-RL ALGORITHM
757758 We provide a formal specification of the Adaptive-Clarification Reinforcement Learning (AC-
759 RL) algorithm. The algorithm operates in an episodic setting where each episode consists
760 of a visual reasoning problem (I, Q) sampled from the dataset \mathcal{D} .
761762 A.1 FORMAL PROBLEM SETUP
763764 Let $\mathcal{M} = (\mathcal{S}, \mathcal{A}, P, R, \gamma)$ denote the Markov Decision Process where:
765766

- $\mathcal{S} = \mathcal{I} \times \mathcal{Q} \times \mathcal{H}$ is the state space,
- $\mathcal{A} = \mathcal{C}$ is the action space (caption generation),
- $P : \mathcal{S} \times \mathcal{A} \rightarrow \Delta(\mathcal{S})$ is the transition kernel,
- $R : \mathcal{T} \rightarrow [0, 1]$ is the reward function defined on trajectories,
- $\gamma = 1$ (undiscounted episodic setting).

772773 A single episode proceeds as follows. At $t = 0$, the vision policy emits the initial caption
774 $c_0 \sim \pi_\theta(\cdot | s_0)$ with $s_0 = (I, Q, \emptyset)$. The reasoner stochastically decides whether to request
775 clarification and, if so, which question to ask; we denote this by a θ -independent kernel
776 $q_1 \sim p(\cdot | s_0, c_0)$. When $q_1 \neq \emptyset$, the clarification caption is produced by a *frozen* checkpoint
777 π_{ref} :

778
$$c_1 \sim \pi_{\text{ref}}(\cdot | s_1), \quad s_1 = (I, Q, \{c_0, q_1\}),$$

779 and the reasoner produces a final answer according to a θ -independent kernel $A \sim p(\cdot |$
780 $Q, c_0, (q_1, c_1))$. When $q_1 = \emptyset$, the reasoner answers from (Q, c_0) directly. The next state
781 appends the sampled variables to the dialogue history. Thus P composes the reasoner's
782 stochastic behavior and the frozen clarification-caption policy π_{ref} ; conditioned on the
783 agent's action c_0 , these post-action mechanisms are θ -*independent* by construction. The
784 episode terminates after the answer A is produced, and the reward is assigned as in the
785 main text.

786 **Clarification captioning is frozen.** In all experiments, the clarification caption c_1 is
787 generated by a *frozen* checkpoint π_{ref} (typically the reference policy). Its distribution does
788 not change during training. Consequently, no gradients flow through π_{ref} or through the
789 reasoner \mathcal{R} ; only the log-probabilities of the initial caption tokens c_0 contribute to the policy
790 update.791 A.2 ADVANTAGE COMPUTATION
792793 We use Beta-Normalization Policy Optimization (BNPO) (Xiao et al., 2025) for advan-
794 tage estimation. BNPO addresses a limitation of standard GRPO: while GRPO uses fixed
795 normalization, BNPO adaptively normalizes rewards using a Beta distribution whose
796 parameters evolve with the policy. This provides lower-variance gradient estimates and more
797 stable training.798 For a group of rewards $\{R^{(i)}\}_{i=1}^M$ from a single prompt, BNPO fits Beta distribution param-
799 eters $(\alpha_\beta, \beta_\beta)$ via method-of-moments from the group statistics, then computes advantages
800 as:

801
$$A_{\text{BNPO}}^{(i)} = \frac{R^{(i)} - \mu_\beta}{\sigma_\beta + \epsilon}, \quad \text{where } \mu_\beta = \frac{\alpha_\beta}{\alpha_\beta + \beta_\beta} \quad (3)$$

802

803 Although BNPO was designed for binary rewards, we found it effective with our ternary
804 reward structure, moderately outperforming standard GRPO in our experiments.
805806 A.3 POLICY UPDATE
807808 The policy is updated using the clipped surrogate objective with a fixed KL reference:
809

810
$$\mathcal{L}_{\text{clip}}(\theta) = -\mathbb{E}_{(s_t, a_t)} [\min(r_t(\theta)A_t, \text{clip}(r_t(\theta), 1 - \epsilon, 1 + \epsilon)A_t)] + \beta D_{KL}(\pi_\theta \| \pi_{\text{ref-KL}}), \quad (4)$$

810 where $r_t(\theta) = \pi_\theta(a_t | s_t)/\pi_{\theta_{\text{old}}}(a_t | s_t)$, and A_t is the advantage computed via BNPO (Xiao
 811 et al., 2025). The gradient is computed solely on the initial captioning segments c_0 ; the
 812 clarification responses c_1 are emitted by the frozen π_{ref} and are thus θ -independent.
 813

814 **A.4 TRAINING ALGORITHM**
 815

816 **Algorithm 1** Adaptive-Clarification Reinforcement Learning (AC-RL)
 817

818 **Require:** Dataset \mathcal{D} , vision model \mathcal{V}_θ , reasoner \mathcal{R} , penalty α , group size M , gradient steps
 819 K

820 1: Initialize policy $\pi_\theta \leftarrow \mathcal{V}_\theta$ with parameters θ
 821 2: Initialize *frozen* clarification captioner π_{ref} (checkpoint used only for c_1)
 822 3: Initialize fixed KL reference $\pi_{\text{ref}} \leftarrow \pi_\theta$
 823 4: **for** iteration $t = 1$ to T **do**
 824 5: Sample batch $\mathcal{B} = \{(I_j, Q_j)\}_{j=1}^B \sim \mathcal{D}$
 825 6: **for** each $(I_j, Q_j) \in \mathcal{B}$ **do**
 826 7: **for** $i = 1$ to M **do**
 827 8: Generate initial caption: $c_0^{(i,j)} \sim \pi_\theta(\cdot | I_j, Q_j)$
 828 9: Sample reasoner's clarification decision: $q_1^{(i,j)} \sim \mathcal{R}_{\text{clarify}}(\cdot | Q_j, c_0^{(i,j)})$ (no
 829 gradients)
 830 10: **if** $q_1^{(i,j)} \neq \emptyset$ **then**
 831 11: Generate clarification caption from *frozen* checkpoint: $c_1^{(i,j)} \sim \pi_{\text{ref}}(\cdot |$
 832 12: $I_j, Q_j, (c_0^{(i,j)}, q_1^{(i,j)})$) (no gradients)
 833 13: Get answer: $A^{(i,j)} \sim \mathcal{R}(\cdot | Q_j, c_0^{(i,j)}, (q_1^{(i,j)}, c_1^{(i,j)}))$ (no gradients)
 834 14: Set clarification flag: $C^{(i,j)} = 1$
 835 15: **else**
 836 16: Get answer: $A^{(i,j)} \sim \mathcal{R}(\cdot | Q_j, c_0^{(i,j)})$ (no gradients)
 837 17: Set clarification flag: $C^{(i,j)} = 0$
 838 18: **end if**
 839 19: **end for**
 840 20: Fit Beta parameters $(\alpha_\beta^{(j)}, \beta_\beta^{(j)})$ to $\{R^{(i,j)}\}_{i=1}^M$
 841 21: Compute BNPO advantages $\{A_{\text{BNPO}}^{(i,j)}\}_{i=1}^M$
 842 22: **end for**
 843 23: **for** $k = 1$ to K **do**
 844 24: Update policy with clipping and KL penalty: $\theta \leftarrow \theta - \eta \nabla_\theta \mathcal{L}_{\text{clip}}(\theta; \pi_{\text{ref-KL}})$
 845 25: **end for**
 846 26: **end for**
 847 27: **return** Trained policy π_θ

851
 852
 853
 854
 855
 856
 857
 858
 859
 860
 861
 862
 863

864 B UNBIASEDNESS OF THE THREE-TIER REWARD
865

866 In this section, we provide a formal proof that our three-tier reward structure maintains
867 the unbiasedness property of the REINFORCE policy gradient estimator, even when the
868 reasoner exhibits stochasticity.

869 **Theorem 1** (Unbiasedness of the Three-Tier Reward with Stochastic Reasoner). *Let $\xi \sim$
870 $p(\cdot | \tau)$ denote all post-action randomness after the policy chooses its actions (e.g., the
871 reasoner's sampling noise and, when clarification is used, the frozen clarification-caption
872 sampling). Define the extended trajectory $\tilde{\tau} = (\tau, \xi)$ with joint density:*

$$873 \quad p_\theta(\tilde{\tau}) = p_\theta(\tau) \cdot p(\xi | \tau) \quad (5)$$

874 where $p(\xi | \tau)$ is independent of θ .

875 Let the tiered reward function be defined as:

$$876 \quad R_{tier}(\tilde{\tau}) = \begin{cases} 1 & \text{if } \text{correct}(A(\tilde{\tau})) \wedge C(\tilde{\tau}) = 0 \\ \alpha & \text{if } \text{correct}(A(\tilde{\tau})) \wedge C(\tilde{\tau}) > 0 \\ 0 & \text{otherwise} \end{cases} \quad (6)$$

877 where $\alpha \in (0, 1)$, and define the training objective:

$$878 \quad J(\theta) = \mathbb{E}_{\tilde{\tau} \sim p_\theta}[R_{tier}(\tilde{\tau})]. \quad (7)$$

879 For any baseline $b_t(s_t)$ that does not depend on the action a_t , the REINFORCE estimator:

$$880 \quad \hat{g}(\tilde{\tau}) = \sum_{t=0}^{T-1} \nabla_\theta \log \pi_\theta(a_t | s_t) \cdot (R_{tier}(\tilde{\tau}) - b_t(s_t)) \quad (8)$$

881 satisfies $\mathbb{E}_{\tilde{\tau} \sim p_\theta}[\hat{g}(\tilde{\tau})] = \nabla_\theta J(\theta)$, i.e., the policy gradient remains unbiased despite the 0/ α /1
882 reward shaping and post-action stochasticity.

883 **Proof. Step 1: Setup.** The extended trajectory $\tilde{\tau} = (\tau, \xi)$ includes both the policy-
884 generated trajectory $\tau = (s_0, a_0, s_1, a_1, \dots, s_T)$ and the post-action randomness ξ . The joint
885 probability decomposes as:

$$886 \quad p_\theta(\tilde{\tau}) = p(s_0) \prod_{t=0}^{T-1} \pi_\theta(a_t | s_t) P(s_{t+1} | s_t, a_t) \cdot p(\xi | \tau), \quad (9)$$

887 where $p(s_0)$ is the initial state distribution, P is the environment transition kernel, and
888 $p(\xi | \tau)$ is the distribution over post-action randomness given the trajectory; by assumption,
889 $p(\xi | \tau)$ is θ -independent.

890 **Step 2: Policy Gradient Theorem.** For $R_{tier}(\tilde{\tau})$,

$$891 \quad \nabla_\theta J(\theta) = \nabla_\theta \int p_\theta(\tau) p(\xi | \tau) R_{tier}(\tilde{\tau}) d\xi d\tau \quad (10)$$

$$892 \quad = \int p_\theta(\tau) p(\xi | \tau) R_{tier}(\tilde{\tau}) \nabla_\theta \log p_\theta(\tau) d\xi d\tau \quad (11)$$

$$893 \quad = \int p_\theta(\tilde{\tau}) R_{tier}(\tilde{\tau}) \nabla_\theta \log p_\theta(\tau) d\tilde{\tau}, \quad (12)$$

894 using that $\nabla_\theta \log p_\theta(\tilde{\tau}) = \nabla_\theta \log p_\theta(\tau) + \nabla_\theta \log p(\xi | \tau)$ and $\nabla_\theta \log p(\xi | \tau) = 0$ by θ -
895 independence. Since $p(s_0)$ and P are θ -independent,

$$896 \quad \nabla_\theta \log p_\theta(\tau) = \sum_{t=0}^{T-1} \nabla_\theta \log \pi_\theta(a_t | s_t), \quad (13)$$

897 hence

$$898 \quad \nabla_\theta J(\theta) = \mathbb{E}_{\tilde{\tau} \sim p_\theta} \left[\sum_{t=0}^{T-1} \nabla_\theta \log \pi_\theta(a_t | s_t) \cdot R_{tier}(\tilde{\tau}) \right]. \quad (14)$$

918 **Step 3: Baseline Subtraction.** For any $b_t(s_t)$ not depending on a_t ,

$$919 \quad \mathbb{E}_{\tilde{\tau} \sim p_\theta} \left[\sum_{t=0}^{T-1} \nabla_\theta \log \pi_\theta(a_t \mid s_t) \cdot b_t(s_t) \right] \quad (15)$$

$$920 \quad = \sum_{t=0}^{T-1} \mathbb{E}_{s_t} [b_t(s_t) \cdot \mathbb{E}_{a_t \sim \pi_\theta(\cdot \mid s_t)} [\nabla_\theta \log \pi_\theta(a_t \mid s_t)]] = 0, \quad (16)$$

921 so

$$922 \quad \mathbb{E}_{\tilde{\tau} \sim p_\theta} \left[\sum_{t=0}^{T-1} \nabla_\theta \log \pi_\theta(a_t \mid s_t) \cdot (R_{\text{tier}}(\tilde{\tau}) - b_t(s_t)) \right] = \nabla_\theta J(\theta). \quad (17)$$

923 \square

924 **Remark 2** (If the reasoner is θ -dependent). *If, instead, $p(\xi \mid \tau)$ depends on θ (e.g., shared trunk), then*

$$925 \quad \nabla_\theta \log p_\theta(\tilde{\tau}) = \sum_t \nabla_\theta \log \pi_\theta(a_t \mid s_t) + \nabla_\theta \log p_\theta(\xi \mid \tau),$$

926 and an unbiased estimator must add the extra score term $\nabla_\theta \log p_\theta(\xi \mid \tau)$ multiplied by the
927 same return. Alternatively, one may stop gradients through the reasoner or generate ξ using
928 frozen modules to enforce θ -independence.

929 **Proposition 3** (Unbiased gradient with θ -dependent reasoner). *If $p_\theta(\xi \mid \tau)$ depends on θ ,
930 then*

$$931 \quad \nabla_\theta J(\theta) = \mathbb{E} \left[\left(\sum_t \nabla_\theta \log \pi_\theta(a_t \mid s_t) + \nabla_\theta \log p_\theta(\xi \mid \tau) \right) R_{\text{tier}}(\tilde{\tau}) \right],$$

932 so the unbiased score-function estimator must include both terms (each may use an appropriate
933 baseline that is independent of the respective sampled variable).

934 **Corollary 4.** *Under the θ -independence of $p(\xi \mid \tau)$, the three-tier reward preserves the
935 unbiasedness of the REINFORCE estimator for $\nabla_\theta J(\theta)$. Algorithms such as PPO, GRPO,
936 and BNPO, which optimize clipped or normalized surrogate objectives, remain applicable with
937 this reward; however, their gradient estimates are generally biased (by design) and converge
938 to stationary points of their respective surrogate objectives rather than guaranteeing an
939 unbiased gradient of $J(\theta)$.*

940
941
942
943
944
945
946
947
948
949
950
951
952
953
954
955
956
957
958
959
960
961
962
963
964
965
966
967
968
969
970
971

972 **C DATASETS AND BASELINES**
973974 We evaluate on seven benchmarks that span diverse visual contexts beyond symbolic math-
975 ematics: natural images, statistical charts, scientific diagrams, tables, real-world scenes,
976 puzzles, and pattern recognition tasks. This diversity ensures our evaluation captures a
977 broad range of visual reasoning challenges.978

- 979 • **MathVista** (testmini) (Lu et al., 2024a): A consolidated benchmark of 1000 examples,
980 covering figure QA, geometry, math word problems, and textbook QA across diverse
981 reasoning types.
- 982 • **MathVision** (Wang et al., 2024): 3040 problems sourced from real math competitions,
983 spanning 16 mathematical disciplines across 5 difficulty levels.
- 984 • **MathVerse** (Zhang et al., 2024): 2612 visual math problems transformed into 6 versions
985 with varying visual vs. textual information to test genuine diagram comprehension.
- 986 • **MMMU** (dev & validation) (Yue et al., 2024): 1050 college-level questions across 6
987 disciplines and 30 image types including charts, diagrams, tables, and scientific figures.
- 988 • **WeMath** (testmini, strict) (Qiao et al., 2024): 1740 visual math problems organized
989 around 67 hierarchical knowledge concepts, decomposing composite problems into sub-
990 problems to assess foundational knowledge.
- 991 • **DynaMath** (worst-case) (Zou et al., 2025): 501 seed questions represented as Python
992 programs generating variants with different numerical values or geometric transforma-
993 tions to test reasoning robustness.
- 994 • **LogicVista** (Xiao et al., 2024): 448 questions evaluating logical reasoning across 5 types
995 (deductive, inductive, spatial, numerical, mechanical) sourced from human IQ and rea-
996 soning test banks.

997998 **Model Baselines.** We compare against leading proprietary models: GPT-4o (Achiam
999 et al., 2023), Claude-3.7-Sonnet, Gemini-2.0-Flash (Team et al., 2023), o1 (Jaech et al.,
1000 2024), Gemini 2.5 Pro (Comanici et al., 2025), and Seed1.5-VL (Guo et al., 2025b);
1001 open-weights general-purpose models: Qwen2.5-VL (Bai et al., 2025) and Ovis2 (Lu
1002 et al., 2024b); and reasoning-optimized models: InternVL3-MPO variants (Zhu et al.,
1003 2025), VL-Rethinker (Wang et al., 2025a), QVQ-72B-Preview (Team, 2024b), and MMR1-
1004 Math (Sicong Leng, 2025).1005 **D GENERATION DIVERSITY DURING TRAINING**
10061008 An interesting emergent property of AC-RL training is that it maintains greater generation
1009 diversity compared to standard binary-reward RL. Figure 4 tracks the fraction of training
1010 batches where all M generated captions receive identical rewards (zero standard deviation),
1011 which serves as an indicator of diversity collapse.1012 Both methods show an upward trend as entropy naturally decreases during policy optimiza-
1013 tion. However, AC-RL consistently maintains a lower fraction of uniform-reward batches
1014 (approximately 0.31 vs 0.42 at convergence). This difference likely stems from the tiered
1015 reward structure: while standard RL only distinguishes between success and failure, AC-
1016 RL’s intermediate reward ($\alpha = 0.7$) creates a richer gradient landscape that encourages the
1017 model to explore different captioning strategies.1018 **E TRAINING DYNAMICS**
10191021 Figure 5 tracks the (smoothed) frequency of clarification requests during training. The
1022 consistent decrease confirms our hypothesis that AC-RL teaches the captioner to front-load
1023 information that would otherwise trigger follow-up questions. Combined with the main-
1024 tained generation diversity shown in Appendix D, this suggests the model finds genuinely
1025 informative captioning strategies rather than mode-collapsing to a narrow set of templates.

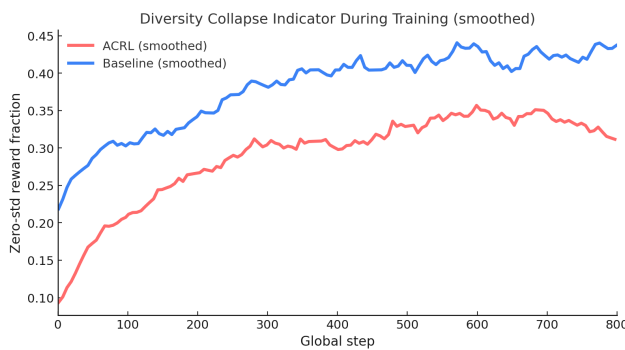


Figure 4: Fraction of uniform-reward batches during training. AC-RL (red) maintains lower values than standard RL (blue), indicating more diverse caption generation throughout training. Both methods show increasing trends as policies converge, but AC-RL's tiered reward structure preserves more exploration.

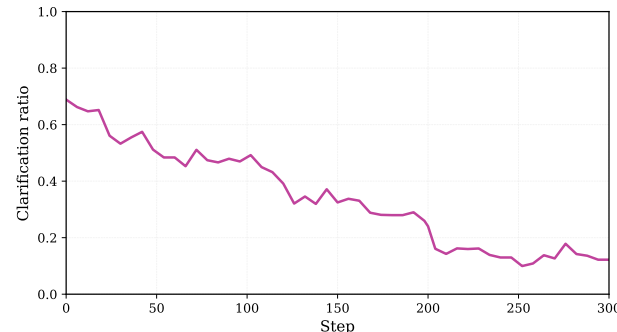


Figure 5: Clarification request frequency during AC-RL training. The rate decreases from approximately 65% at initialization to 20% at convergence, demonstrating that the model learns to produce more self-sufficient initial captions.

1080 **F QUALITATIVE CAPTION COMPARISONS**
10811082 To illustrate how AC-RL modifies captioning behavior, we present a representative example
1083 comparing captions from the pretrained baseline and AC-RL on a table-reading problem
1084 (Figure 6).
1085

1086	oval beads	\$2/kilogram
1087	rectangular beads	\$3/kilogram
1088	star-shaped beads	\$2/kilogram
1089	spherical beads	\$2/kilogram
1090	heart-shaped beads	\$3/kilogram
1091	square beads	\$2/kilogram
1092	flower-shaped beads	\$2/kilogram

1097
1098 **Question:** Chase wants to buy 4 kilograms of oval beads and 5 kilograms
1099 of star-shaped beads. How much will he spend? (Unit: \$)
11001101 **Baseline Caption**1102
1103 The image appears to be a table listing
1104 various types of beads along with their
1105 respective prices per kilogram. The table
1106 has two columns and lists different
1107 types of beads available for purchase.
1108 I can see oval beads, rectangular
1109 beads, star-shaped beads, spherical
1110 beads, heart-shaped beads, square
1111 beads, and flower-shaped beads. Each
1112 type has a corresponding price per kilo-
1113 gram shown in the second column. The
1114 table appears to be from a craft supply
1115 store or similar retailer.
11161117 **AC-RL Caption**1118 The image appears to be a table
1119 listing various types of beads along
1120 with their respective prices per kilo-
1121 gram. The table is as follows:
1122

1123 Beads	1124 Price/kg
oval beads	\$2
rectangular beads	\$3
star-shaped beads	\$2
spherical beads	\$2
heart-shaped beads	\$3
square beads	\$2
flower-shaped beads	\$2

(Model outputs Markdown; rendered for readability.)

1125 Figure 6: Qualitative comparison on a table-reading problem. The baseline describes the
1126 table structure but omits numerical values. AC-RL extracts all prices needed to compute
1127 the answer.
11281129 The baseline caption correctly identifies the table structure and all bead types, but refers
1130 to prices abstractly without extracting the actual values. AC-RL, having learned from
1131 clarification requests during training that numerical details are essential, extracts every
1132 price explicitly.
11331134 **G PROMPT TEMPLATES**1135 We present the complete set of prompts used in our AC-RL framework. The prompts are
1136 structured to maintain clear role separation between the captioner (visual description) and
1137 reasoner (problem-solving), while enabling controlled interaction during training.
11381139 **G.1 VISION-LANGUAGE MODEL PROMPTS**1140 **Initial Caption Generation.** The following prompt instructs the VLM to generate com-
1141 prehensive visual descriptions without solving the problem:
1142

```

1134
1135 vlm_initial_description_prompt
1136
1137 I need your help analyzing this image to prepare for answering the following
1138 question:
1139 {question}
1140 IMPORTANT: DO NOT answer the question directly. Instead, provide a
1141 comprehensive and detailed description of everything visible in the image
1142 that could be relevant for answering this question.
1143 Focus on describing:
1144
1145     • All objects, people, text, and visual elements in the image
1146     • Spatial relationships between different elements
1147     • Any text content that is visible, transcribed exactly
1148     • Colors, shapes, patterns, and visual attributes
1149     • Relevant contextual details and background information
1150
1151 Your description should be detailed enough that someone could mentally
1152 reconstruct the image without seeing it, but DO NOT provide step-by-step
1153 instructions on how to recreate it.

```

1154

1155 **Clarification Response.** When the reasoner requests specific visual information, the

1156 frozen reference model uses this prompt:

```

1156 vlm_focused_description_prompt
1157
1158 Original Question: {question}
1159 Previous Description: {previous_descriptions}
1160 CONTEXT: The description above was provided for this image, but some details
1161 might be missing or unclear. We are asking this specific follow-up question
1162 to gather additional visual details.
1163 Your specific task: {focus_request}
1164 CRITICAL INSTRUCTIONS:
1165
1166     • You are a VISUAL DESCRIPTOR only - DO NOT attempt to answer the
1167     original question
1168     • DO NOT solve the problem or provide calculations
1169     • DO NOT give step-by-step solutions or reasoning
1170     • ONLY describe what you can see in the image that relates to the
1171     specific request
1172     • Focus solely on visual elements: objects, text, numbers, shapes,
1173     spatial relationships
1174     • If asked about measurements, describe what you see but don't
1175     calculate or solve
1176     • If asked about equations, transcribe what's visible but don't solve
1177     them
1178     • Be thorough and precise in your description since this is to clarify
1179     specific missing details

```

```

1180
1181
1182
1183
1184
1185
1186
1187

```

1188 G.2 REASONER PROMPTS
11891190 **Adaptive Decision Mechanism.** The reasoner evaluates whether the initial caption is
1191 sufficient or requires clarification:

```

1192
1193     reasoner_adaptive_decision_prompt
1194
1195     You are an expert visual reasoning assistant. Your task is to analyze the
1196     given image description and decide if you can solve the problem directly or
1197     if you need one specific piece of additional visual information.
1198     Image Description: {description}
1199     Question: {question}
1200     ANALYSIS INSTRUCTIONS:
1201
1202     1. CAREFUL EVALUATION: Analyze if the description contains all specific
1203     visual details needed to solve completely and accurately.
1204
1205     2. BE CONSERVATIVE: If missing ANY crucial visual detail, request MORE
1206     information rather than guess.
1207
1208     3. ONE CLARIFICATION ONLY: You can request specific additional visual
1209     information if needed.
1210
1211     4. DECISION CRITERIA:
1212
1213         • If you have ALL visual details needed: Status = SOLVED
1214         • If missing crucial visual information: Status = NEED_MORE_INFO
1215
1216     5. AVOID ASSUMPTIONS: Don't guess numbers, assume "typical" values, or
1217     fill in missing details.
1218
1219     CRITICAL PRINCIPLES:
1220
1221         • BE SPECIFIC in requests: Ask for exact details you need
1222         • SOLVE CONFIDENTLY when possible: If you have enough information,
1223             provide the complete solution
1224         • REQUEST STRATEGICALLY: Make your one request count - ask for the most
1225             crucial missing details
1226
1227     OUTPUT FORMAT (all fields required):
1228     Reasoning: [Your detailed analysis of what information you have and what
1229     might be missing]
1230     Status: [SOLVED or NEED_MORE_INFO]
1231     Answer: [Your complete final answer if Status is SOLVED - use \boxed{answer}
1232     format, otherwise N/A]
1233     Request: [Your specific request for additional visual information if Status
1234     is NEED_MORE_INFO, otherwise N/A]
1235
1236
1237
1238
1239
1240
1241

```

1242 **Final Answer Generation.** For both direct solving and post-clarification scenarios:
 1243

```

 1244   reasoner_final_prompt
 1245
 1246     You are an expert mathematical reasoning assistant. Based on the complete
 1247     image description below, please solve the mathematical problem step-by-step.
 1248     Complete Image Description: {description}
 1249     Question: {question}
 1250     INSTRUCTIONS:
 1251       1. Analyze the complete image description carefully
 1252       2. Work through the problem step-by-step with clear mathematical
 1253         reasoning
 1254       3. Show all calculations and logical steps
 1255       4. Provide your final answer in the required format
 1256       5. Use \boxed{answer} notation. For multiple choice, use \boxed{letter}
 1257         format
 1258     You MUST follow this format:
 1259     <think>
 1260     Your detailed reasoning and thought process here...
 1261     </think>
 1262     <answer> Final Answer: your final answer here </answer>
 1263
 1264
 1265
```

H TRAINING HYPERPARAMETERS

1266 We provide complete hyperparameter specifications to ensure reproducibility. All experiments
 1267 use the same random seed for dataset sampling to enable fair comparisons.

1268
 1269 Table 8: Hyperparameter settings for AC-RL training across different model sizes.
 1270

Hyperparameter	2B Models	3B Models
<i>Optimization</i>		
Learning rate	3×10^{-6}	2×10^{-6}
Effective batch size	256	256
KL divergence weight (β)	0.001	0.001
<i>LoRA Configuration</i>		
LoRA rank (r)	128	256
LoRA alpha (α)	256	512
LoRA dropout	0.05	0.05
<i>BNPO Settings</i>		
Group size (M)	8	8
Number of iterations	6	6
Remaining parameters	TRL library defaults	
<i>Generation Parameters</i>		
Captioner temperature	1.0	
Captioner max tokens	800	
Reasoner temperature	0.6	
Reasoner top- p	0.95	
Reasoner max tokens	100,000	
<i>Reward Configuration</i>		
Clarification penalty ($1 - \alpha$)	0.3	

1294 **Implementation Details.** We implement AC-RL using the Transformers Reinforcement
 1295 Learning (TRL) library von Werra et al. (2020) with Beta-Normalization Policy Optimiza-

1296 tion (BNPO). The LoRA Hu et al. adapters are applied to all linear layers in the vision-
1297 language models. Training typically converges within 1,000 steps on the ViRL-39K dataset.
1298 All experiments use mixed precision training (fp16).

1299

1300 **Computational Requirements.** Training a 3B parameter captioner with AC-RL re-
1301 quires approximately 50 hours on 8 NVIDIA A6000-Ada GPUs. The 2B models require 40
1302 hours on the same hardware configuration. The reasoner is hosted on a 4× AMD MI250X
1303 node, though it is never fully saturated during training.

1304

1305 I LLM USAGE STATEMENT

1306

1307 We used large language models for grammatical corrections and rewording suggestions to
1308 improve clarity. All research ideas, experimental design, analysis, and scientific contributions
1309 are the original work of the authors. LLMs were not used for generating research content
1310 or results interpretation.

1311

1312

1313

1314

1315

1316

1317

1318

1319

1320

1321

1322

1323

1324

1325

1326

1327

1328

1329

1330

1331

1332

1333

1334

1335

1336

1337

1338

1339

1340

1341

1342

1343

1344

1345

1346

1347

1348

1349